

# Object-based Method for Identifying New Constructions around Water Reservoirs: Preliminary Results

Nayereh Hamidishad  
Institute of Mathematics and Statistics  
University of Sao Paulo  
Email: nhamidi@ime.usp.br

Roberto M. Cesar-Jr  
Institute of Mathematics and Statistics  
University of Sao Paulo  
Email: rmcasar@usp.br

**Abstract**—Identifying new constructions in large cities can be done simply, quickly, and at low cost by applying image processing techniques on time-series remote sensing (RS) images and producing land cover maps. In recent years, object-based (OB) image classification has attracted significant attention as a method for land cover mapping. This method consists of two steps: segmentation and classification. In this research, we will develop a new approach based on image processing techniques to be utilized in the OB classification method for the analysis of urban growth. In this approach, we propose a multi-phase segmentation for the segmentation step and a rule-based method for the classification step. Besides speeding up the process of OB classification, the accuracy of the final preliminary results is another advantage of the proposed approach. Moreover, for collecting RS images, a two-zoom level data collection is adopted using an open source RGB RS database. An important application of analyzing RS images is the detection of non-authorized communities formation around water reservoirs. Therefore, in our preliminary experiments, we selected three different regions around Guarapiranga reservoir in Sao Paulo, Brazil, for collecting our RS images.

**Index Terms**—Image processing, land cover mapping, remote sensing, object-based method.

## I. INTRODUCTION

RS is a technology that involves the use of space-imaging systems for monitoring earth resources and obtaining information from a target through the analysis of acquired data [1]. By development of RS technology, a large number of satellite and aerial images with high quality have been created. The spatial resolution of some of these RS images is improved to centimeters [2].

One way for obtaining satellite images is by utilizing Google Earth Pro<sup>©</sup> software<sup>1</sup>. The database of this software contains high-resolution images of many different areas on the earth [4]. Besides containing an open database of RS images, the availability of historical images and flexibility in selecting different zoom levels and spatial resolutions are the other advantages of this software.

Utilizing RS images for land cover mapping has been widely accomplished using pixel-based approaches, where each pixel is independently classified [5]. Even so, with the increase in spatial resolution of satellite images, a single pixel does not capture well the characteristics of targeted objects and it causes a reduction in the accuracy of classification using pixel-based methods [3].

In contrast with pixel-based methods, OB classification methods are less sensitive to spectral variances within objects and can make use of both object features and spatial relations between objects. Because of these reasons, it has become the main approach in dealing with high-resolution satellite imagery [6]. Many studies compared these two classification methods and concluded that the OB method is more precise in comparison with the pixel-based method [7]. The process of OB classification which is implemented in many studies [8], [9], consists of two steps: segmentation and classification. One of the most commonly used algorithms for segmenting and classifying RS images are multi-resolution segmentation and rule-based classification respectively. However, the multi-resolution segmentation method requires users to determine a set of proper segmentation parameters. In addition, the most important parameter in the multi-resolution segmentation (called scale) can differ between various objects in an image. Moreover, many studies have concluded that to achieve an accurate segmentation result, the multi-scale segmentation method is necessary (i.e., defining a different scale parameter for each class in the scene) [8], [10]. Among the different methods for assessing the values of these parameters, visual assessment is the most common one employed [11]. Therefore, determining and assessing these parameters utilizing the most commonly used methods are very time-consuming. On the other hand, implementing the rule-based method for classifying, especially when the dataset consisting of several large RS images, is also time-consuming. However, utilizing this method may lead to the best results [12]. Additionally, the reservoir objects have similar spectral properties to other objects that cause misclassification of this land cover type. This paper addresses these issues by proposing a new pipeline for the OB classification. It avoids setting a different scale parameter for each class type by implementing a multi-phase segmentation method instead of the multi-scale method. The proposed pipeline also avoids selecting segmentation parameters and classification criteria and threshold values through trial and error on large RS images (that cover larger ground regions and consequently, consist of more objects). Moreover, it classifies the scene in two phases: the reservoir classification and the remained objects classification.

In order to illustrate the performance of the proposed approach, the preliminary results of its application in land

<sup>1</sup><https://www.google.com/earth/desktop/>

cover change detection are presented. We are particularly interested in land cover change detection in regions around water reservoirs. Such changes may be an early indicator of unauthorized and clandestine constructions that may lead to some public problems such as water contamination and precarious housing that may put people in dangerous housing [13].

## II. PROPOSED APPROACH

The flowchart of the proposed approach is illustrated in Figure 1. Its steps are explained in the following subsections.

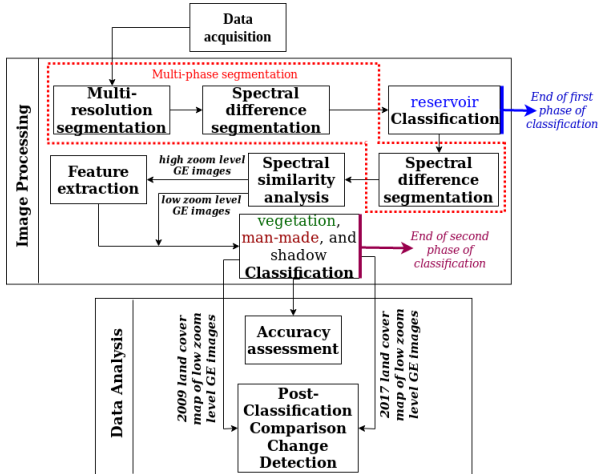


Fig. 1: Flowchart of the proposed approach

### A. Data Acquisition

RS images are provided via Google Earth Pro 7.3.1. For each studied region, in the first, an image with an eye altitude of 2 km is collected. Then, for each GE 2 km sample, an image with an eye altitude of 1 km at the same date, which covers a sub-region that contains all land cover types, is collected. In Figure 2, two GE images that are collected with two different zoom levels from a region around the reservoir are illustrated.

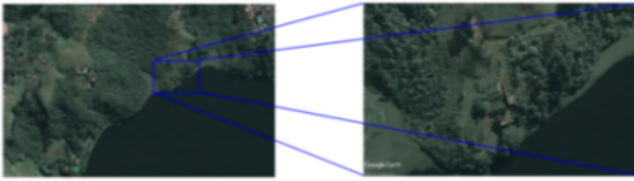


Fig. 2: Illustration of two GE images collected with different zoom levels.

### B. Image Processing

In this study, four land cover types are determined: man-made, vegetation, reservoir, and shadow. The image processing steps are explained in the following.

**Multi-resolution segmentation** The multi-resolution segmentation method essentially identifies single image segments of one pixel and then merges every segment with

its neighbors based on a relative homogeneity criterion. The homogeneity criterion, which is a combination of spectral and shape criteria, besides the scale, constitute the most important parameters in the multi-resolution segmentation. The homogeneity criterion can be customized by weighting color and shape (that is based on compactness and smoothness) criteria [14].

We firstly segmented images with the higher zoom level (or with an eye altitude of 1 km, that are smaller than high eye altitude images more than four times) with different scales, shape and compactness factors and compared segmentation results by visual inspection. When the scale, shape, and compactness parameters are 35, 0.7 and 0.5 respectively, every segment is internally homogeneous and all pixels within it belongs to one class. Then, all GE images with the lower zoom level (or with an eye altitude of 2 km) are segmented utilizing computed factors.

**Spectral difference segmentation** Spectral difference segmentation merges image segments produced by the previous step when the difference between their mean intensities is below the value given by the maximum spectral difference [14]. Applying this method causes a high reduction in the number of segments, especially over the reservoir objects and constructs a segment in each GE image that covers almost the whole reservoir. The advantage of implementing the proposed multi-phase segmentation is that it constructs the purposed segments (segments with sizes close to the sizes of objects in the scene) without needing of setting different set of parameters for each land cover type. This is analogous to some selective attention based methods that may be found in the literature.

**Reservoir classification** The second step is classifying segments obtained from the segmentation step. In this study, a rule-based method is implemented. As mentioned before, implementing the multi-phase segmentation was significantly effective in obtaining segments with sizes close to sizes of the reservoirs objects in the GE images. It made possible to classify the reservoirs segments just utilizing "segment area" and "relative border to the reservoir" features.

**Spectral difference segmentation** Before detecting the other classes of interest, to reduce the number of segments, to merge segments that have low spectral differences and belong to the same classes, and consequently to construct purposed segments, spectral difference segmentation is applied one more time.

**Spectral similarity analysis** In order to analyze the spectral similarities between segments of the same classes in different GE images quickly, a new step is implemented. In this step, the nearest neighbor classifier is applied to all GE images. The segments of one of the GE images with high zoom level are selected as training samples. Regarding our experimental tests, we decided to classify the GE images of each year separately to achieve better results.

**Feature extraction** In order to extract the features that can separate segments of different classes, a group of samples that covers all possible segments in all classes (from GE images with the higher zoom level) is constructed for each

year. Then, using these samples, for every two classes the histograms of features are constructed. Finally, the features with small histogram overlap between classes (brightness, standard deviation, number of pixels/length, quantile, and also customized features,  $R - G$  and  $(R - B)^2 - (R - G)^2$ , where R, G, and B represent mean value of Red, Green, and Blue bands of segments respectively) are selected to be used for the classification.

**Vegetation, man-made, and shadow classification** The necessary rules and related applied thresholds for classifying have been adopted using GE images with the higher zoom level. These are then applied to the GE images with the lower zoom level. The higher zoom level images consist of significantly smaller numbers of segments. It causes the process of adopting rules to be much simpler.

### III. DATA ANALYSIS AND PRELIMINARY EXPERIMENTAL RESULTS

The segmentation and classification steps are implemented using eCognition Developer 9.3.1 software. The accuracy assessment results and change detection maps are obtained using Python.

#### A. Dataset

Twelve GE images are provided from three different regions around Guarapiranga reservoir. These GE images belong to two different years, 2009 and 2017, and have spatial resolutions about 0.3 m.

#### B. Validation and Accuracy Assessment

The land cover map of each GE image is individually assessed using a number of independent validation points, which are generated by a stratified random sampling scheme. Due to the lack of survey points in the studied areas, 250 independent points (with a minimum number of 50 points from each land cover type) and 500 independent points (with a minimum number of 100 points from each land cover type) are randomly generated from the land cover maps of high and low zoom levels images, respectively. The overall accuracies of obtained land cover maps from the GE images with the high and low zoom levels are from 88%-93% and from 93%-94% respectively, and Kappa coefficients are from 84%-90% and from 84%-92% respectively. The accuracy assessment results are computed using one run of the sampling and evaluation procedure.

#### C. Post-classification comparison change detection

One of the most widely used change detection methods is land cover mapping of time-series RS images and then comparing derived land cover maps. This method is called post-classification comparison change detection [4]. In this paper, a change detection matrix for each studied region using the land cover maps of low zoom level images is constructed. Then, utilizing change detection matrices, land cover change maps are produced.

#### D. Preliminary Experimental Results

Figure 3, shows an example of the GE images (which is captured in 2017 with the lower zoom level from the first studied region) and the results of applying all steps of the proposed method. As is illustrated in Figure 3c, after applying the spectral difference segmentation method on Figure 3b, a segment is generated that covers almost the whole reservoir. The result of applying spectral difference segmentation for the second time is illustrated in Figure 3e. We can see the high reduction in the number of segments and the creation of segments which are closer to the real objects. In Figures 3f and 3h, an example of the GE images (which is captured in 2009 with the lower zoom level from the first studied region) and its derived land cover map are illustrated respectively. Comparison of proportions of man-made class in the derived land cover maps shows that the man-made areas in the studied regions are increased up to 400% from 2009-2017. In Figure 3i, the result of post-classification comparison change detection, which is derived by comparing 3f and 3h, is illustrated. In this Figure, important "from-to" change classes are highlighted: from vegetation to man-made (green), from shadow to man-made (white), and from man-made to man-made (red). As illustrated in this change detection map, a high percentage (87%) of new man-made areas were vegetation in 2009. Furthermore, 68% and 29% of the new man-made areas were vegetation in 2009 in the second and third studied regions. These percentages show environmental degradation around Guarapiranga reservoir.

### IV. CONCLUSION

In this study, a data collection using two zoom levels is adopted. Also, instead of the multi-scale segmentation, a multi-phase segmentation method is implemented. In addition to achieving to the purposed segments more quickly (because of elimination of computing a scale parameter for each land cover type), satisfactory results of the classification step is the other advantage of the proposed method. Moreover, segmentation parameters and necessary rules for classifying have been adopted by combining the literature review and visual examination on the GE images with the higher zoom level and then are applied to the GE images with the lower zoom level. This method can significantly decrease the necessary time for obtaining the desired results when we assess segmentation parameters visually and classify segments using the rule-based method. Furthermore, classifying objects is performed in two phases to increase the accuracy of produced land cover maps. Our ongoing work includes the formation of a larger dataset around important water reservoirs in the state of Sao Paulo. This larger dataset will allow us to assess and to improve the proposed approach in a systematic manner. As part of this ongoing work, we will compare the proposed approach to some state-of-the-art, such as [15], [16], [8], [9].

### ACKNOWLEDGMENT

The authors are grateful to FAPESP 2015/22308-2, CNPq and CAPES for funding support.

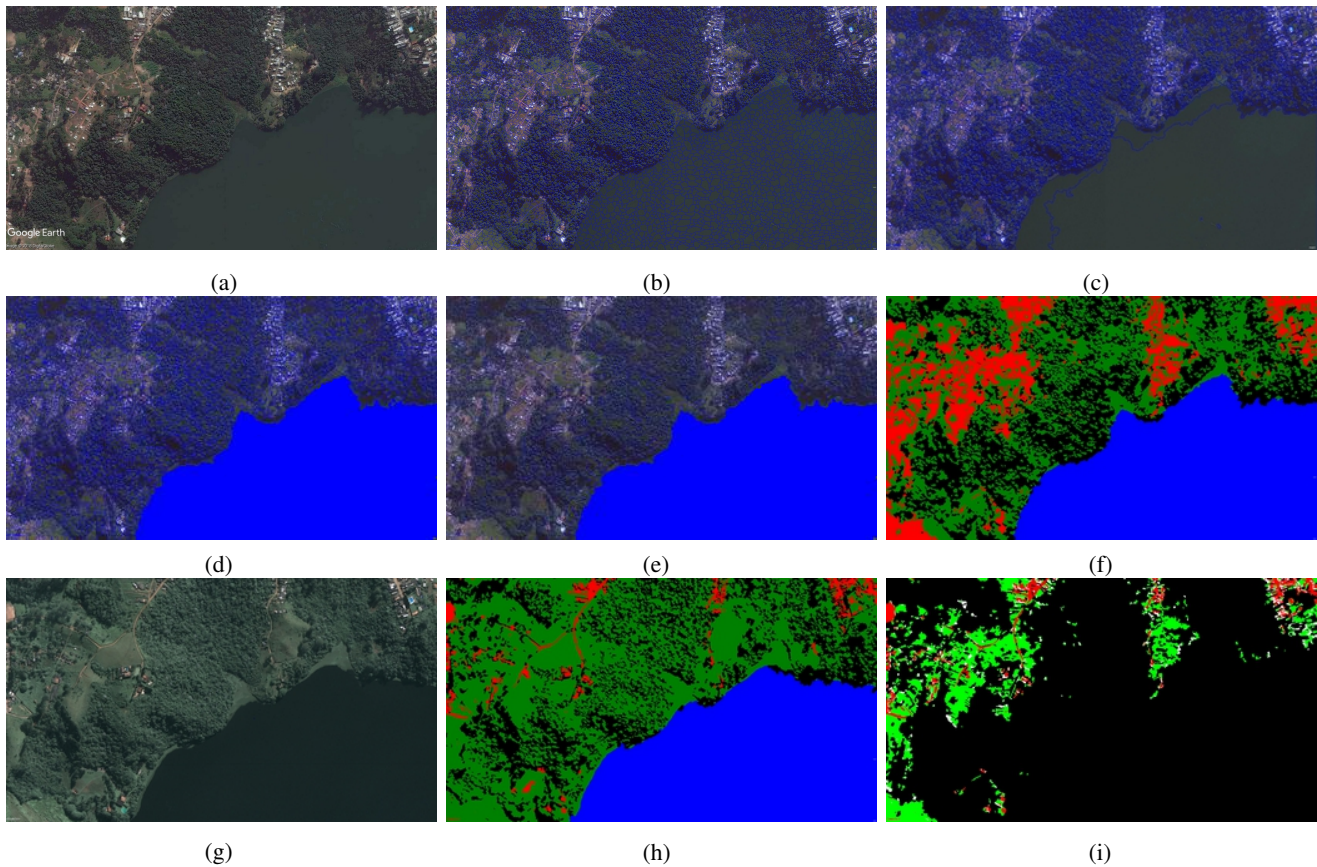


Fig. 3: (a) An example of the GE images (it is captured in 2017 with the lower zoom level from the first studied region); (b) Result of applying the multi-resolution segmentation on (a); (c) Result of applying the spectral difference segmentation on (b); (d) Derived thematic map after classifying reservoir; (e) Result of applying the spectral difference segmentation on the unclassified objects; (f) Land cover map derived from (a); (g) An example of the GE images (it is captured in 2009 with the lower zoom level from the first studied region); (h) Land cover map derived from (g); (i) derived land cover change map from comparing (f) and (h).

## REFERENCES

- [1] N. E. Rozanda, M. Ismail, and I. Permana, "Segmentation google earth imagery using k-means clustering and normalized rgb color space," in *Computational Intelligence in Data Mining-Volume 1*. Springer, pp. 375-386, 2015.
- [2] Y.-T. Liao, "Hierarchical segmentation framework for identifying natural vegetation: a case study of the tehachapi mountains, california," *Remote Sensing*, vol. 6, no. 8, pp. 7276-7302, 2014.
- [3] Q. Hu, W. Wu, T. Xia, Q. Yu, P. Yang, Z. Li, and Q. Song, "Exploring the use of google earth imagery and object-based methods in land use/cover mapping," *Remote Sensing*, vol. 5, no. 11, pp. 6026-6042, 2013.
- [4] J. R. Jensen, *Introductory digital image processing: a remote sensing perspective*, 2015.
- [5] A. El Garouani, D. J. Mulla, S. El Garouani, and J. Knight, "Analysis of urban growth and sprawl from remote sensing data: Case of fez, morocco," *International Journal of Sustainable Built Environment*, vol. 6, no. 1, pp. 160-169, 2017.
- [6] T. Blaschke, G. J. Hay, M. Kelly, S. Lang, P. Hofmann, E. Addink, R. Q. Feitosa, F. Van der Meer, H. Van der Werff, F. Van Coillie et al., "Geographic object-based image analysis towards a new paradigm," *ISPRS journal of photogrammetry and remote sensing*, vol. 87, pp. 180-191, 2014.
- [7] S. W. Myint, P. Gober, A. Brazel, S. Grossman-Clarke, and Q. Weng, "Per-pixel vs. object-based classification of urban land cover extraction using high spatial resolution imagery," *Remote sensing of environment*, vol. 115, no. 5, pp. 1145-1161, 2011.
- [8] E. M. Silveira, S. H. G. Silva, F. W. Acerbi-Junior, M. C. Carvalho, L. M. T. Carvalho, J. R. S. Scolforo, and M. A. Wulder, "Object-based random forest modelling of aboveground forest biomass outperforms a pixel-based approach in a heterogeneous and mountain tropical environment," *International Journal of Applied Earth Observation and Geoinformation*, vol. 78, pp. 175188, 2019.
- [9] C. A. d. Silva Junior, M. R. Nanni, J. F. d. Oliveira-Junior, E. Cezar, P. E. Teodoro, R. C. Delgado, L. S. Shiratsuchi, M. Shakir, and M. L. Chicati, "Object-based image analysis supported by data mining to discriminate large areas of soybean," *International journal of digital earth*, vol. 12, no. 3, pp. 270292, 2019.
- [10] H. Tong, T. Maxwell, Y. Zhang, and V. Dey, "A supervised and fuzzy based approach to determine optimal multi-resolution image segmentation parameters," *Photogrammetric Engineering Remote Sensing*, vol. 78, no. 10, pp. 10291044, 2012.
- [11] H. Zhang, J. E. Fritts, and S. A. Goldman, "Image segmentation evaluation: A survey of unsupervised methods," *Computer Vision and Image Understanding*, vol. 110, no. 2, pp. 260280, may 2008.
- [12] Z. Ziaei, B. Pradhan, and S. B. Mansor, "A rule-based parameter aided with object-based classification approach for extraction of building and roads from worldview-2 images," *Geocarto International*, vol. 29, no. 5, pp. 554569, 2014.
- [13] T. Kruse, "Crime organizado coordena invasões em áreas de mananciais de so paulo," <https://sustentabilidade.estadao.com.br/noticias/geral,crime-organizado-coordena-invasoes-em-areas-de-mananciais-de-sao-paulo,70002884543>.
- [14] eCognition Developer 9.3.1 User Guide, Trimble Germany GmbH, 2018.
- [15] A. Whyte, K. P. Ferentinos, and G. P. Petropoulos, "A new synergistic approach for monitoring wetlands using sentinel-1 and 2 data with object-based machine learning algorithms," *Environmental Modelling Software*, vol. 104, pp. 4054, 2018.
- [16] S. Liu, Z. Qi, X. Li, and A. G.-O. Yeh, "Integration of convolutional neural networks and object-based post-classification refinement for land use and land cover mapping with optical and sar data," *Remote Sensing*, vol. 11, no. 6, p. 690, 2019.